

MODELLING OF SOLID-STATE TRANSFORMER TO SUPPORT THE INTERCONNECTION OF MICROGRIDS FOR POWER SHARING AND HARMONIC COMPENSATION DURING ISLANDED OPERATION

Mayaka N. Moses^{1,*}, Michael J. Saulo²

¹Jomo Kenyatta University of Agriculture and Technology, Nairobi, Kenya.

²Technical University of Mombasa, Msa, Kenya.

*Corresponding Author: Mayaka N. Moses (Email: Mosmay60@gmail.com)

(Received: 11-December-2023; accepted: 10-February-2024; published: 31-March-2024)

<http://dx.doi.org/10.55579/jaec.202481.447>

Abstract. *The concept of microgrids has gained popularity in the distribution of electricity to the final consumer. Microgrids integrating energy storage devices, combined heat and power systems (CHP), and renewable energy generation are especially becoming attractive to industrial consumers – such as industrial parks – due to environmental and economic benefits. However, the intermittence of renewable energy sources implies that storage is essential for economic operation. Furthermore, technological limitations of storage solutions for the grid imply that we need to consider supplying the power to the main grid. Grids are also designed for unidirectional operation, which implies that microgrids cannot receive and send power to the grid. This research paper shows the potential for Solid State Transformers (SSTs) to support power-sharing among islanded microgrids. The microgrids are interconnected through the low-voltage medium, which implies that they can send and receive power from the main grid. Simulations through MATLAB demonstrate that the SST can support the integration of renewable energy sources at the low-voltage Direct Current (DC) bus. Furthermore, advanced controls – particularly, particle swarm optimization – can be implemented to mitigate harmonics (only 1.17% in the presence of non-linear loads and 0.36% in the pres-*

ence of resistive loads alone) and voltage imbalance (the voltage unbalance factor is less than 1%) at the microgrid level. Microgrids generating excess power can also share with neighboring microgrids in the absence of the main grid (for instance, during a fault). This research is instrumental in reconfiguring conventional grids to meet the needs of modern power system requirements.

Keywords: *Microgrids, Solid state transformers, Renewable energy sources, Harmonics control, Particle swarm optimization*

1. Introduction

The electric power industry is constantly evolving to address increasing and dynamic load demand, power production, and delivery challenges. This constant evolution means the electrical grid of the future will look drastically different from today's hierarchical, centralized system [1]. With the growing need for reliable, affordable, efficient, and cleaner energy, the power industry must grow and adjust to ensure future needs are met. One approach that is gaining momentum in the electric power industry is the

concept of microgrids. A microgrid is a group of interconnected loads and distributed energy resources, which act as a single controllable bounded system. Microgrids can operate independently or in conjunction with the main electrical grid [2]. They bring together diverse engineering disciplines including distributed generation, renewable generation integration, smart grid/automation, advanced control and communications, and energy management systems to meet some of today's most prevalent energy challenges [3].

Microgrids can eliminate inconsistencies in energy supply and reduce greenhouse gas emissions through the integration of renewable energy sources. Regardless of their benefits, there is an issue with power storage since the availability of renewable energy sources can result in the generation of excess electricity. This surplus electricity, often referred to as excess energy, can be stored in energy storage systems like batteries or even exported back to the main grid [4]. However, exporting to the main grid is not permitted because the traditional grid operates on a unidirectional flow of power, with electricity flowing from large-scale power plants to consumers [5]. As such, a microgrid can only operate in a single direction – supplying power to the grid or receiving power from the grid. As such, microgrids can only feed power to the main grid without receiving power from the grid. Based on these limitations, there is a need for the development of effective schemes, which can enable microgrids to receive power from the main grid (when the local resources are not sufficient or economic) while at the same time supplying power to the main grid when there is excess energy in the local microgrid.

In this research, SSTs are proposed as a potential approach for interconnecting microgrids through the medium voltage grid so that they can both receive power from the grid and supply excess power to other microgrids. From the literature, there is evidence that SSTs can be used to interconnect microgrids for various purposes such as interconnecting microgrids with different voltage and frequency levels [6, 7], interface of renewable energy sources [8], and interconnection of Alternating Current (AC) and DC microgrids [9]. Building on the literature, the

present research aims to demonstrate that SSTs can be used to interconnect multiple microgrids through the medium voltage grid so that they can either receive power or deliver power to the medium voltage grid. Furthermore, through appropriate controls through the SSTs, the issues of harmonics can be addressed to enhance the performance of microgrids. For demonstrations, a Proportional–Resonant (PR) controller with selective harmonic compensation is proposed to address the harmonics in the microgrid configuration. The implemented controller is also designed to ensure balanced voltage in the three phases even when single-phase loads are connected. To ensure optimal performance, the PR controller and its selective harmonic compensators are tuned using particle swarm optimization.

2. Materials and Methods

In this research, two microgrids are interfaced to the medium voltage grid through SSTs. An SST is a high-frequency power transformer, which is isolated by the AC-to-AC conversion technique. The SST is composed of a Full bridge multilevel rectifier for converting AC to DC, a dual active bridge, which is a DC-DC converter, and a three-phase inverter, which converts DC voltage to AC voltage as shown in Fig. 1. In this paper, interfacing of the renewable energy sources and microgrids is achieved through a three-level neutral point clamped (NPC) inverter. As such, harmonic issues and voltage balancing are achieved through the control of the inverter. An LCL(inductor-capacitor-inductor) filter is used at the output of the inverter to achieve the desired signals. Regarding the selection of the PR compensator gain values, an online optimization is done using a Particle Swarm Optimization (PSO) algorithm. All renewable energy sources are connected to the low voltage (LV) DC link capacitor. In this case, when there is no sufficient local energy, power can flow from the medium voltage grid to the microgrid through the SST. In the absence of the main grid or excess production, the local microgrid is fed through the inverter while excess power is fed back to the grid through the DC-DC converter

and rectifier. As such, the rectifier and Dual Active Bridge (DAB) can operate in both boost and buck mode while the inverter operates only in the buck mode.

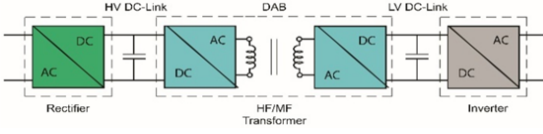


Fig. 1: Solid state transformer.

2.1. Rectifier Model

The rectifier is a single-phase converter for generating a DC voltage. A model of a single cell of the rectifier (there are three cells for each phase) for buck operation is presented in Fig. 2. In the boost mode, R_{Load} is replaced with a DC source while $v_{(ph-MV)}$ becomes the output voltage. In this work, the rectifier model was developed using four Metal-oxide Semiconductor Field Effect Transistors (MOSFETs), a capacitor, a resistor, and an inductor. For three-phase power, the single rectifier cells were designed to feed into single-cell DAB. Applying the Kirchhoff laws,

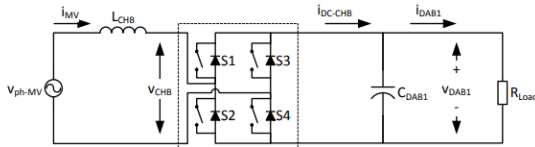


Fig. 2: Single H-bridge cell.

the current and voltage transfer functions of the rectifier can be derived as follows

$$G_{idq-CHB} = -\frac{v_{DAB1}(sL_{CHB} + R_{CHB})}{(sL_{CHB} + R_{CHB})^2 + \omega_g^2 L_{CHB}^2} \quad (1)$$

$$G_{vid-CHB} = -\frac{D_{d-CHB}(sL_{CHB} + R_{CHB}) - D_{d-CHB}L_{CHB}\omega_g}{D_{d-CHB}^2 + 3sC_{DAB1}(sL_{CHB} + R_{CHB})} \quad (2)$$

$$G_{vid-MV} = -D_{d-CHB} * v_{DAB1} \quad (3)$$

1) DAB Model

The DC-DC converter is a DAB, which converts DC voltage from one level to another. A model of a single cell of the DAB is shown in

Fig.3. The model was assembled using independent components (MOSFETS, transformer, inductor, and capacitor). In the buck mode, the DAB converts high DC voltage (v_{DAB1}) to a low DC voltage (v_{DAB2}). In the Boost mode, the DAB converts low DC voltage (v_{DAB2}) into a high DC voltage (v_{DAB1}). A key point to note is that the values of the inductor in buck mode are divided by the transformation ratio to obtain the value of the inductor in the boost mode (as such $L_{-DAB-boost} = \eta_{Tr}^2 / L_{-DAB-back}$). Furthermore, In the boost mode, V_{DAB2} becomes the input voltage while v_{DAB1} becomes the output voltage. Similar to the rectifier, Kirchhoff

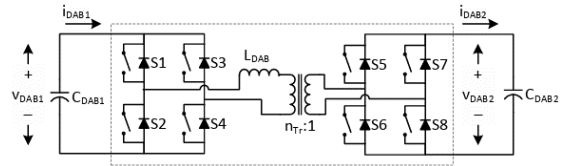


Fig. 3: Model of the DAB.

laws are applied to obtain the current and voltage transfer functions of the DAB as follows

$$G_{id-DAB-buck} = -\frac{2v_{DAB2}}{\eta_{Tr}^{-2}(sL_{DAB} + R_{DAB})} \quad (4)$$

$$G_{vi-DAB} = \frac{R_{L2}(-2D_{DAB} + 1)}{sR_{L1}C_{DAB2} + 1} \quad (5)$$

2) Inverter Model

The three-level Neutral Point Clamped (NPC) inverter converts low DC power to AC power for supply to the local loads. The model of the three-level NPC inverter is presented in Fig. 4. Similar to the other models, the inverter model was assembled using independent components (MOSFETs, resistors, inductors, and capacitors). Based on the control objectives of the inverter, it is evident that the output filter is the primary way through which harmonics are suppressed. As such, the LCL is assumed to be the plant in developing the controllers of the inverter. The transfer function of the LCL filter with a damping resistor (the resistor is used to reduce resonance and improve stability) is shown in equation 6 [10]. The transfer function links the output current to the voltage of the NPC

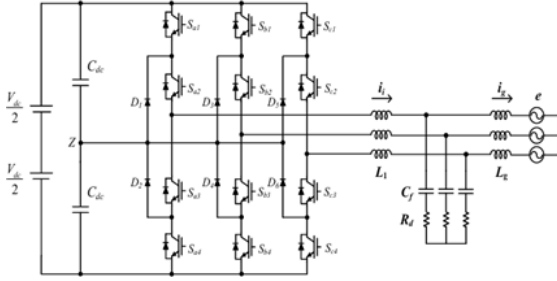


Fig. 4: The model of three-level NPC inverter.

inverter. The parameters of the LCL filter can be obtained using the guidelines provided in [11].

$$G_f(s) = \frac{s^2 + s \left(\frac{R_d}{L_g} \right) + \left(\frac{1}{L_g C_f} \right)}{L_i s^3 + s^2 \left(\frac{(L_i + L_g) R_d}{L_g} \right) + s \left(\frac{(L_i + L_g)}{L_g C_f} \right)} \quad (6)$$

To control the harmonics of the LCL filter, a PR controller is used as shown in Fig.3. The transfer function of the PR controller as well as associated harmonics is presented in equation 7 [12].

$$G_{PR}(s) = k_p + k_i \frac{2w_c s}{s^2 + 2w_c s + w_0^2} + \sum_{h=3.5.7} k_{ih} \frac{2w_c s}{s^2 + 2w_c s + (hw_0)^2} \quad (7)$$

2.2. Control of the Rectifier

For the rectifier, in the boost mode, the current and voltage injected into the medium grid are controlled. The voltage through the filter inductor is measured and compared with the reference value (smooth sinusoidal wave) to generate an error, which is fed to a Proportional Integral (PI) controller to generate the reference current as shown in Fig.5. The reference current signal is then compared with the current measured to generate an error signal. Through a PI controller, the duty cycle for controlling the rectifier is generated. In the buck mode, the input current and DC voltage are controlled. The voltage control loop is used to control the DC voltage by comparing the desired value and the DC value. The resulting error is fed into a PI controller to generate a reference current, which is compared with the measured current value and

passed through a PI controller to generate the duty cycle.

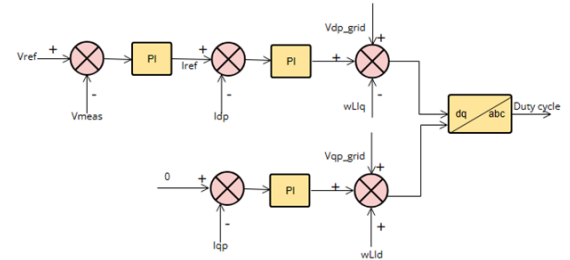


Fig. 5: Controllers of the CHB.

2.3. Control of the DAB

Similar to the CHB, the DAB is controlled through the current control method with an inner current loop and an outer voltage loop. The inner current controller is shown in Fig.6. A key point to note is that the controllers of the DAB are almost similar in both boost and buck modes. The only difference is the reference point, in this case, the high voltage link voltage and current measurements are used in the boost mode while the measurements in the low voltage link are used in the buck mode.

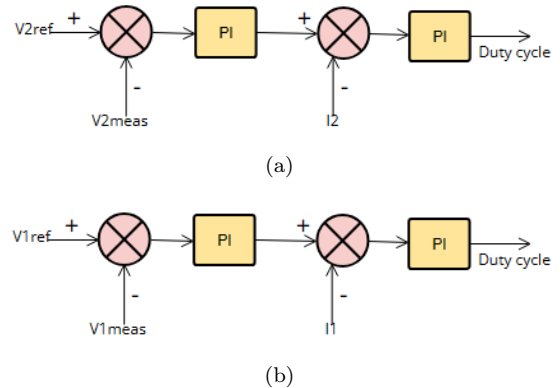


Fig. 6: Controllers of the DAB: (a) buck mode and (b) boost mode.

2.4. Control of the Inverter

Finally, the 3-level inverter is controlled through the current control method. The control objec-

tive of the inverter is to limit harmonics, balance voltage, and generate an AC power output. In this case, the key parameters controlled are the NPC output voltage and current as well as the load voltage and current. As shown below, Fig.7 is used to generate the reference values for the third, fifth, and seventh harmonics as well as the fundamental frequency harmonics. The outputs are summed, compared with the grid current, and the error is fed into the PSO-tuned PR controller as shown in Fig.8. The outputs of Figs.

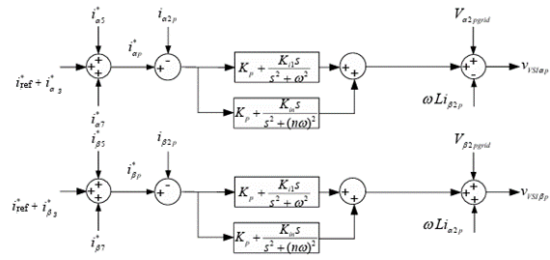


Fig. 8: PR controller.

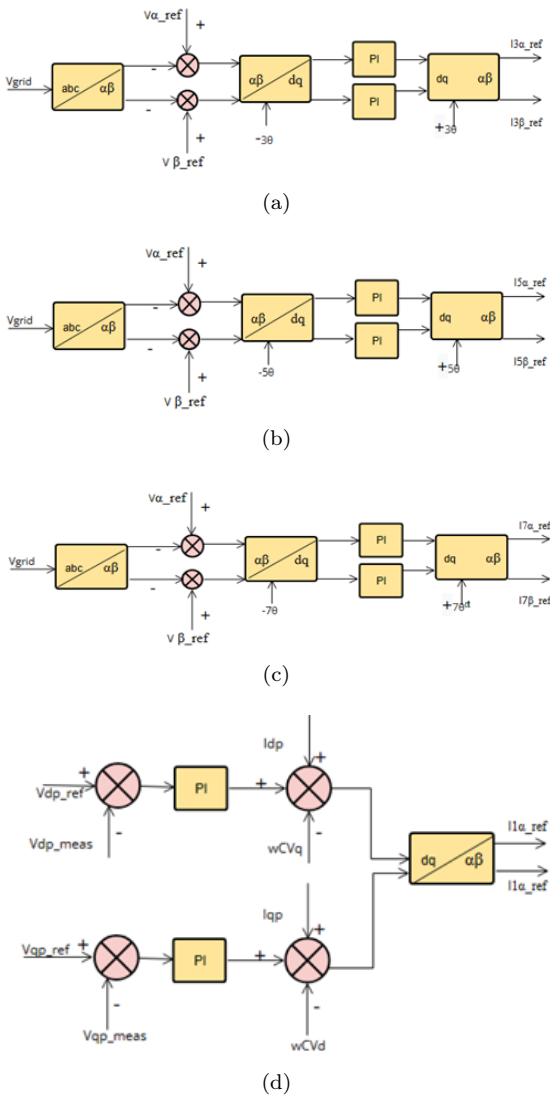


Fig. 7: Generating the reference current values: (a) reference for third, (b) fifth, (c) seventh, and (d) fundamental harmonics.

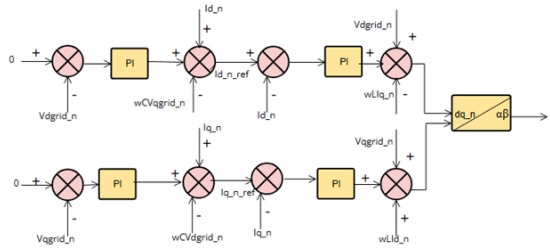


Fig. 9: The control scheme of the negative sequence component.

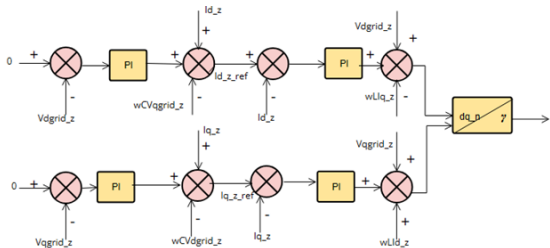


Fig. 10: The control scheme of the zero-sequence component.

8,9 and 10 are summed and then converted to abc to generate the duty cycle of the 3-level NPC inverter.

3. Results and Discussion

To verify the performance of the proposed controllers, the SST was designed as described in the modeling section. The overall model and associated control structures are shown in Figs 3 and 4 below. The medium grid voltage was set to 13,200 V. The low voltage DC-link voltage was set to 393 V with a target root mean square (RMS) voltage of 220 V. The other parameters of the system are presented in Table 1. Regard-

ing renewable energy sources, existing models of a Battery Energy Storage System (BESS) and solar power system were used to generate 50 kV of power at a voltage level of 393 V.

Following the development of the proposed controllers and implementation of the models, the overall project was developed as shown in Fig. 11. In this case, the Institute of Electrical and Electronics Engineers (IEEE) 34 Node Test Feeder [24.9 kV] was modified and used to link three microgrids. The system was customized to have a voltage of 13.2 kV, which is the voltage level of the distribution system. As such, microgrids were directly connected to the medium voltage grid through the SST. The Point of Common Coupling (PCC) of the microgrid group was located at node 832. This study modifies the IEEE 34 test Feeder model by adding three microgrids downstream from the PCC, each at nodes 890, 842, and 860.

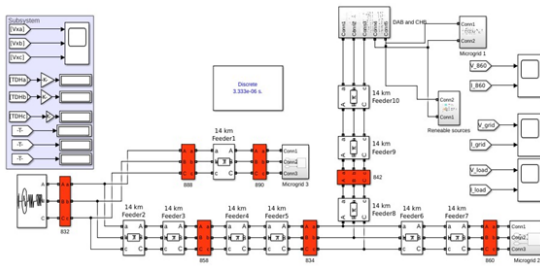


Fig. 11: The overall simulation models.

3.1. Grid-Connected Mode

In the grid-connected mode, the microgrids were designed to receive power from the medium voltage grid. In this mode of operation, the power demand was met from the main grid while the power generated from renewable energy sources was stored in the battery energy storage system. It is, however, important to notice that the voltage of the low DC link was maintained at the required value (393 V) through the BESS. In the absence of this approach, it could be difficult to model and control all system dynamics, which affect voltage control. Based on this approach, the voltage profile of the load feeder is shown in Fig. 12. Similarly, the current profile of the load is shown in Fig. 12. Finally, the power output of

the SST is shown in Fig. 13. Overall, the results show that the SST can reliably be used to support power flow from the medium voltage grid to the loads while at the same time providing a mechanism for addressing harmonics.

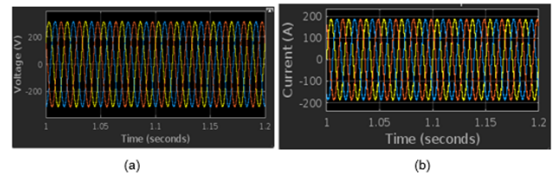


Fig. 12: (a) voltage profile and (b) current profile.

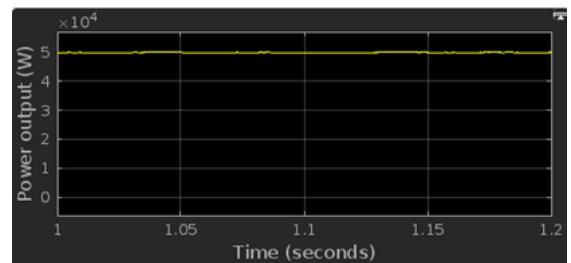


Fig. 13: Power output in the grid-connected mode for microgrid 1.

3.2. Islanded Operation

Intentional islanding of the interconnected microgrids was initiated so that they operate independently of the main grid. The islanded microgrids were designed to share power – immediately after islanding – depending on local demand. In this case, one microgrid was designed to deliver power to another microgrid through the medium voltage grid. In both the buck and boost modes, the controllers were able to achieve the expected DC power in the intermittent stages of the SST as shown in Fig. 14a,b. The average DC voltage at the high-voltage DC link was found to be 11,393 V while that of the low-voltage DC link was about 393 V. In addition to the DC voltage, controllers were implemented to generate AC power for the loads and the medium voltage grid. The voltage of the point of common coupling was found to be 13.2 kV as shown in Fig. 15a. Similarly, the power from renewable energy sources was used to meet

Tab. 1: The parameters used in the simulation

| Parameter | Value |
|--|-----------------------|
| Phase voltage in Medium voltage grid | 13200 V |
| Input inductance of H-bridge | $50e^{-3}$ mH |
| Input resistance of H-bridge = $120 \cdot \pi \cdot L_{HB} \cdot 0.05$ | 0.942 Ω |
| Input capacitance of H-bridge = $50000 / (0.6 \cdot 60 \cdot \pi \cdot (11397^2))$ | 3.404 μF |
| Load resistance at the output of H-bridge = $11397^2 / (50e^3 / 3)$ | 7793.496 Ω |
| Switching frequency of H-bridge | $15e^3$ Hz |
| Medium voltage of DAB | 11397 |
| Nominal Power | $50e^3$ W |
| Low voltage of DAB | 393 V |
| The transformation ratio of the transformer | 29 |
| Switching frequency of DAB | $30e^3$ Hz |
| Inductor of DAB | 28.950 mH |
| Resistor of DAB | 545.694 Ω |
| Minimum voltage of DAB in Buck | 11345.005 V |
| Minimum voltage of DAB in Boost | 360.252 V |
| Capacitor of DAB in Buck | 0.216 μF |
| Capacitor of DAB in Boost | 214.034 μF |
| DAB load resistor in Buck | 9.267 Ω |
| DAB load resistor in Boost | 7793.496 Ω |

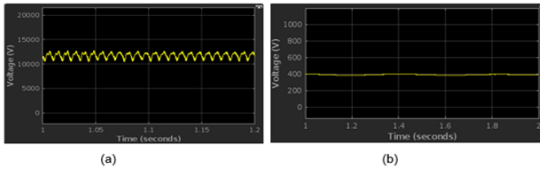


Fig. 14: DC voltage: (a) high voltage link and (b) low voltage link.

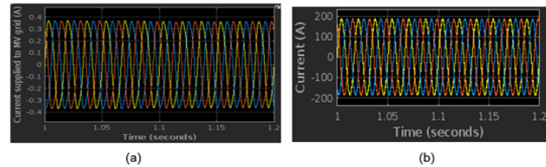


Fig. 16: (a) Current supplied to the medium voltage grid and (b) current supplied to the loads through the inverter.

the local demand while at the same time meeting the demand for the second microgrid. The renewable energy sources were able to produce power with an output voltage of 220 V RMS as shown in Fig. 15b. The current profiles of the point of common coupling and the loads are shown in Fig. 16a-b, respectively. A key point

to note is that the implemented controllers were effective in balancing the voltage of the three phases even in the presence of non-linear single-phase loads. This is evident from the amplitudes of the three phases, which are almost the same.

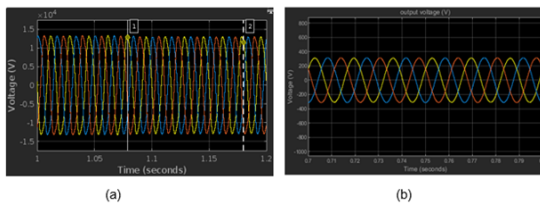


Fig. 15: The voltage waveform of power supplied to the medium voltage grid and (b) the voltage waveform for power supplied to the local loads.

3.3. Harmonics Control

In the first scenario, a simulation was carried out using only PI controllers to verify the presence of harmonics in the model as shown in Fig. 17a. From the results, the THD of 27.3% is very high in relation to the IEEE standards. The fifth- and seventh-order harmonics also violate the specified limits. In the second scenario, the performance of PSO-tuned PR controllers was

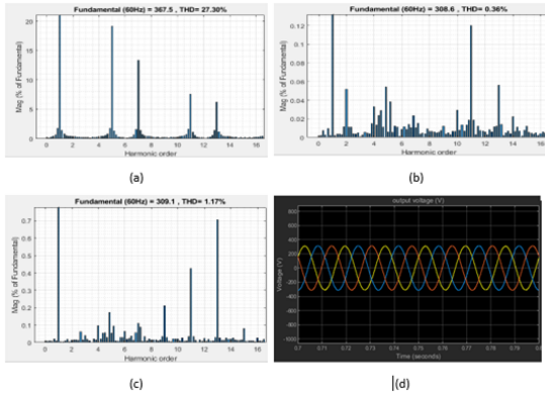


Fig. 17: Harmonic compensation in a microgrid: (a) Without a controller, (b) PSO-tuned PR controller without non-linear loads, (c) SISO-tuned PR controller with non-linear loads, and (d) Output voltage waveform.

evaluated in the absence of nonlinear loads. The output harmonic spectrums are presented in Fig. 17b. From the figure, it can be seen that the controller can eliminate harmonics (0.36%). In this final scenario, single-phase non-linear loads were added to each of the three phases. The results obtained for the PSO-tuned PR controller show that the THD is 1.17% (the third, fifth, and seventh-order harmonics are 0.06%, 0.18%, and 0.08%, respectively). These findings can be compared to those obtained in the literature as follows: As shown in Table 2, the proposed scheme outperforms the existing schemes in most of the comparison metrics. Only the research by [1] shows superior performance under linear loads. However, since power systems mainly serve non-linear loads, it can be suggested that the proposed scheme is superior.

4. Conclusions and Recommendations for Future Research

The objective of this research was to implement an SST to support the interconnection of microgrids through the medium voltage grid. In this case, multiple controllers were implemented to address various objectives including suppressing harmonics (PSO-tuned PR con-

troller), voltage balance, and bidirectional power flow (to support power-sharing among microgrids during the islanded mode. Based on MATLAB/SIMULINK simulations, the following conclusions can be drawn:

- The SST can be used to interconnect microgrids so that they can share power through the medium voltage grid during the islanded mode of operation as shown in Figs.10-13.
- The PR compensator can provide efficient harmonics compensation. The IEEE 519 standard specifies that THD in systems below 69 kV should be limited to 5% with each harmonic limited to 3%. In this research, the THD was found to be 0.36% and 1.17% for simple resistive loads and non-linear loads respectively.
- The sequence-component control scheme can be able to balance the voltage of the load. Particularly, the voltage unbalance was limited to 3% as specified in the American National Standard for Electric Power Systems and Equipment (ANSI) C84.1.
- The PSO-tuned PR controller achieved better results in terms of harmonic suppression as compared to the schemes proposed in the literature in most of the measures.

Regardless of the findings presented in this research, there are some areas that could require additional research. First, there is a need to study the economic dispatch of various energy sources to optimize the economic performance of microgrids interconnected with the main grid. Second, there is a need to study the power protection schemes, which can be used to support the implemented system architecture. This could include the study of stability analysis of the architecture as well as the coordination of the power protection devices.

References

- [1] Biju, K. & Ramchand, R. (2020). An adaptive control strategy for single-phase cascaded H-bridge multilevel inverter under

Tab. 2: Comparison of the findings with those available in the literature

| Author | Proposed Scheme | THD (%) | | Third Harmonic order (%) | Fifth Harmonic order (%) | Seventh Harmonic order (%) |
|------------------|---|-------------|-----------------|--------------------------|--------------------------|----------------------------|
| | | Linear Load | Non-linear Load | | | |
| [1] | multi-resonant controller | 0.26 | 2.42 | | | |
| [13] | PR controller tuned through the Single Input/Single Output (SISO) method | | | 0.613 | 0.474 | 0.338 |
| [6] | PR controller tuned through PSO, Grey Wolf Optimization, and Harris Hawks' Optimization | 2.94 | | | | |
| [10] | hybrid asynchronous PSO Newton-Raphson algorithm | | 8.56 | | | |
| [11] | Asynchronous PSO Genetic algorithm based selective harmonic elimination (SHE) | 0.90 | | | | |
| [12] | Flower Pollination Algorithm-optimized SHE | | 2.36 | 0.28 | 0.15 | 0.12 |
| Present research | PR controller tuned through PSO with voltage balancing | 0.36 | 0.17 | 0.06 | 0.18 | 0.08 |

distorted load conditions. *Electrical Engineering*, 102, 1051–1062.

- [2] Zhang, F., Zhao, H., & Hong, M. (2015). Operation of networked microgrids in a distribution system. *CSEE Journal of Power and Energy Systems*, 1, 12–21.
- [3] Burkes, K., Cordaro, J., Keister, T., & Cheung, K. (2017). Solid state power substation roadmap. *US Department of Energy, Washington, DC*.
- [4] Ebrahim, M.A., Aziz, B.A., Nashed, M.N., & Osman, F.A. (2021). Optimal design of proportional-resonant controller and its harmonic compensators for grid-integrated renewable energy sources based three-phase voltage source inverters. *IET Generation, Transmission & Distribution*, 15, 1371–1386.
- [5] Savaghebi, M., Jalilian, A., Vasquez, J.C., & Guerrero, J.M. (2012). Secondary control for voltage quality enhancement in microgrids. *IEEE Transactions on Smart Grid*, 3, 1893–1902.
- [6] Malik, S.M., Sun, Y., & Hu, J. (2022). A novel solid-state transformer-based control topology for interconnected MV and LV hybrid microgrids. *Energy Reports*, 8, 10385–10394.
- [7] Rashidi, M., Nasiri, A., & Cuzner, R. (2016). Application of multi-port solid state transformers for microgrid-based distribution systems. *IEEE International Conference on Renewable Energy Research and Applications (ICRERA)*, 605–610.
- [8] Zheng, L., Kandula, R.P., & Divan, D. (2021). Current-source solid-state DC transformer integrating LVDC microgrid, energy storage, and renewable energy into MVDC grid. *IEEE Transactions on Power Electronics*, 37, 1044–1058.
- [9] Zolfaghari, M., Gharehpetian, G.B., Shafiekhah, M., & Catalão, J.P. (2022). Comprehensive review on the strategies for controlling the interconnection of AC and DC microgrids. *International Journal of Electrical Power & Energy Systems*, 136, 107742.
- [10] Memon, M.A., Mekhilef, S., & Mubin, M. (2018). Selective harmonic elimination in multilevel inverter using hybrid APSO algorithm. *IET Power Electronics*, 11, 1673–1680.
- [11] Memon, M.A., Siddique, M.D., Mekhilef, S., & Mubin, M. (2021). Asynchronous particle swarm optimization-genetic algorithm (APSO-GA) based selective harmonic elimination in a cascaded H-bridge multilevel inverter. *IEEE Transactions on Industrial Electronics*, 69, 1477–1487.
- [12] Panda, K.P., Bana, P.R., & Panda, G. (2020). FPA optimized selective harmonic elimination in symmetric-asymmetric reduced switch cascaded multilevel inverter.

IEEE transactions on industry applications, 56, 2862–2870.

- [13] Zammit, D., Staines, C.S., Apap, M., & Licari, J. (2017). Design of PR current control with selective harmonic compensators using Matlab. *Journal of Electrical Systems and Information Technology*, 4, 347–358.

About Authors

Michael Juma SAULO is a Doctorate degree holder in Electrical Power Systems Engineering from University of Cape Town South Africa (2014). A career researcher, Senior lecturer and Registrar in charge of Partnership, Research and Innovation at Technical University of

Mombasa (TUM). His passion for teaching and research has resulted in a number of project supervision at undergraduate/postgraduate level and several publications in refereed journals. His main field of research include among others; Electrical Power Systems analysis, planning and design and Renewable Energy studies. He can be contacted through michaelsaulo@tum.ac.ke.

Mayaka N. MOSES is a Master's student in Electrical Engineering at Jomo Kenyatta University of Agriculture and Technology. His main research interests include power security studies, renewable energy integration, power system planning, and artificial intelligence. He can be contacted through mosmay60@gmail.com.